

Analysis of the $J^P=1^+$ three-pion system using a generalized Watson theorem for production of multi-quark states

R. S. Longacre

Brookhaven National Laboratory, Upton, New York 11976

(Received 16 October 1981; revised manuscript received 12 March 1982)

We analyze the $J^P=1^+$ three-pion production amplitudes obtained from the most recent diffractive, charge-exchange, and backward-production experiments. We have found effects in the amplitudes that we interpret in terms of $q\bar{q}$, $q^2\bar{q}^2$, and $q^3\bar{q}^3$ interactions. The $q\bar{q}$ piece gives rise to the A_1 resonance whose parameters are $M_{A_1}=1230\pm 30$ MeV and $\Gamma_{A_1}=330\pm 60$ MeV, whereas the backward-production reaction shows a strong $q\bar{q}$ and $q^2\bar{q}^2$ interference effect. The $\epsilon\pi$ scattering couples only to the $q^2\bar{q}^2$ and $q^3\bar{q}^3$, and thus argues in favor of Jaffe's four-quark model of the ϵ .

I. INTRODUCTION

In the present paper we introduce a generalization of the Watson theorem, first derived by Aitchison,¹ and apply it to the analyses of the diffractive reaction $\pi^-p\rightarrow(3\pi)p$,² the charge-exchange reaction $\pi^-p\rightarrow(3\pi)n$,³ and the backward-production reaction $K^-p\rightarrow\Sigma(3\pi)$,⁴ which include $\rho\pi$ and $\epsilon\pi$ production. The present work supersedes an earlier paper.⁵ However, many details will not be repeated in this paper and will rely on the earlier paper.

The main purpose of the work presented here is to shed additional light on two questions that arose from previous work.⁵⁻⁸ These two questions are as follows: Why does the A_1 production cross section peak up at lower mass (1100 MeV) in almost all reactions (except high- t diffractive production), while a detailed analysis gives a higher A_1 mass, 1250 MeV? What is the true nature of the so-called Deck mechanism⁹ and can one unify its treatment with the production of quark states? All previous work⁵⁻⁸ has answered the first question and has sidestepped the second question. In our attempt to address the second question, we obtain a dual approach that parametrizes the problem in terms $q\bar{q}$, $2q^2\bar{q}^2$, and $3q^3\bar{q}^3$ poles. The pattern of coupling of these poles argues strongly in favor of Jaffe's four-quark model of the ϵ .¹⁰

The paper is divided up into four sections. In Sec. II we introduce the generalized Watson theorem of Aitchison and discuss its application in Refs. 5 through 8. Section III deals with a detailed fit to the 1^+ $\rho\pi$ and $\epsilon\pi$ amplitudes coming from diffractive,² charge-exchange,³ and backward-production⁴ channels. In order to obtain

a fit three K -matrix poles are necessary. These poles have a natural interpretation in terms of the two-quark ($q\bar{q}$), four-quark ($2q^2\bar{q}^2$), and six-quark ($3q^3\bar{q}^3$) states. We further argue that the multi-quark poles are dual to the background terms of the previous analyses.⁵⁻⁸

II. GENERALIZED WATSON THEOREM

The problem of how one should parametrize the production amplitudes for two-particle systems was first solved by using the Watson theorem, which related the physics of production to the physics of formation. The theorem uses the propagation and decay of intermediate states as determined by two-particle formation experiments through a phase-shift parametrization (i.e., $e^{i\delta}\sin\delta$). The recipe is to take full production amplitudes as a product of two factors. The first describes the production process and the second, the propagation and decay of a particular two-body state which scatters with phase shift δ . The Watson factor W_f is the formation amplitude with phase space and formation barrier divided out, i.e., two-body T matrix:

$$W_f = \frac{e^{i\delta}\sin\delta}{q^{l+1}}. \quad (2.1)$$

However for diffractive production, double particle exchange was proposed as the dominant effect and led to the model of Deck.⁹

Aitchison was able to combine production mechanisms like the Deck effect with resonance propagation by introducing a K -matrix formalism which is a natural generalization of the Watson theorem. One can achieve a unitary two-body for-

mation T matrix for the description of intermediate states by a K -matrix approach:

$$T = (1 - iK)^{-1}K. \quad (2.2)$$

A relationship between poles in the K matrix and Breit-Wigner parameters is given in the Appendix. As shown by Aitchison the two factors of Eq. (2.2) play two distinct roles. The $(1 - iK)^{-1}$ term describes the propagation of two-body intermediate states, while the K term governs the formation and decay of these states. A notation which we pursue in the Appendix gives the K matrix for n poles formed in channel α and decaying in channel β as

$$K_{\alpha\beta} = \sum_{j=1}^n \pm \frac{(m_j \Gamma_{j\alpha})^{1/2} (m_j \Gamma_{j\beta})^{1/2}}{m_j^2 - s}, \quad (2.3)$$

where the \pm depends on the signs of the couplings. The generalization that Aitchison achieved was to simply replace the $(m_j \Gamma_{j\alpha})^{1/2}$ term by a complex number which represents the production strength of the intermediate state. Thus by defining a P vector

$$P_\beta = \sum_{j=1}^n \frac{C_j (m_j \Gamma_{j\beta})^{1/2}}{m_j^2 - s}, \quad (2.4)$$

one can write the production amplitudes

$$T = (1 - iK)^{-1}P. \quad (2.5)$$

Additional terms such as the Deck amplitude can be added to the P vector.

The most extensive application of the above formalism was to the $3\pi J^P=1^+$ system.⁵⁻⁸ Most works only considered the $\rho\pi$ S -wave channel for diffractive production and introduced only one K -matrix pole plus a Deck background which appears in the P vector. References 5 and 6 introduced an additional K -matrix pole which played only a minor role in the diffractive channel. However, Ref. 5 pointed out the importance of this additional pole when one includes charge-exchange data, which contains ρ exchange and thus analyzes the $\rho\pi$ formation channel directly. The presence of this background term in the K -matrix was interpreted as a $2q2\bar{q}$ state proposed by Jaffe.¹⁰

In the next section we again pursue the analysis of the $3\pi 1^+$ system with the idea of having the same poles in the P vector as in the K matrix and thus generating the Deck amplitude out of these poles. For comparison with this type of fit we will use our previous analysis⁵ where the Deck amplitude was only included in the P vector and not the K matrix.

III. THREE- K -MATRIX-POLE FIT TO THE $J^P=1^+$ 3π SYSTEM

In this section we simultaneously apply the K -matrix formalism to the low- t [$0.0-0.05$ (GeV/c)²] and high- t [$0.05-0.7$ (GeV/c)²] diffractive data of ACCMOR,² along with the backward baryon-exchange (BEX) data,⁴ and also including the charge-exchange (CEX) data.³ The $1^+\rho\pi$ state can be either in an S wave or a D wave. However, no substantial D wave has been observed in the three analyses above. The ACCMOR analysis which by far has the greatest statistical significance, observes the 1^+ D wave down to a factor of 20. For this analysis we have left out the D wave, but if one should extend the analysis out past 1.5 GeV (which we do not) one should include the D -wave contribution. A clear and comparatively narrow peak does appear around 1.65 GeV in the D wave, where ACCMOR observes a ratio of S to D of the same order of magnitude.

Let us consider the number of parameters involved in the fit that we present in this paper. In order to describe well the above-mentioned amplitudes, we need three K -matrix poles and thus three masses along with two couplings corresponding to $\rho\pi$ and $\epsilon\pi$ decay modes (nine parameters). The $\Gamma_{j\alpha}$ of Eq. (2.3) for the ρ and ϵ couplings are as follows. We have for the S -wave $\rho\pi$ channel,

$$\Gamma_{j\rho} = q_{\rho\pi} \gamma_{j\rho}^2, \quad (3.1)$$

and for the ρ -wave $\epsilon\pi$ channel,

$$\Gamma_{j\epsilon} = q_{\epsilon\pi}^3 \gamma_{j\epsilon}^2. \quad (3.2)$$

The $q_{\rho\pi}$ and $q_{\epsilon\pi}$ are the cm momenta of the $\rho\pi$ and $\epsilon\pi$, respectively.

The number of production parameters of the P vector [(Eq. (2.4)] necessary for the ACCMOR low- t (LT) data are three complex C_i^{LT} , one for each K -matrix pole. The same number is necessary for high- t (HT) ACCMOR data making 12 parameters for diffractive production. For the CEX data, we will only consider the spin-flip natural-exchange amplitude. This amplitude is assumed to be dominated by ρ exchange and thus represents a true picture of $\rho\pi$ scattering (this same assumption was used in our earlier paper⁵). We can achieve this old-style Watson theorem by writing the P vector as

$$P_\alpha^{\text{CEX}} = C^{\text{CEX}} \sum_{j=1}^3 \frac{(m_j \Gamma_{j\alpha})^{1/2}}{m_j^2 - s}, \quad (3.3)$$

where C^{CEX} is a complex number, thus two additional parameters.

Finally, in principle the BEX data should add three more complex C_i^{BEX} , giving a total of 29 parameters. However, some of these parameters become very small during the fit to the above-described data. This is due primarily to the very interesting difference the ACCMOR and the CEX amplitudes, which have by far the most data and the smallest errors. This difference is the total lack of $\epsilon\pi$ amplitudes in the CEX data and the comparatively large amount of $\epsilon\pi$ in the ACCMOR data. This asymmetry picks out one K -matrix pole to describe the $\epsilon\pi$ data almost exclusively. The other interesting feature involves the most important contribution to all the data, the A_1 resonance. The A_1 ends up being totally decoupled from the $\epsilon\pi$ channel and is described mostly by one K -matrix pole. These properties of the fit can best be understood in terms of Jaffe's explanation of the nature of the ϵ itself. Jaffe¹⁰ has claimed the ϵ and its SU(3) partners, the S^* and the δ resonances, are really $2q2\bar{q}$ states. Therefore the K -matrix pole that decays only into $\epsilon\pi$ is naturally associated with a $3q3\bar{q}$ state, since it cannot decay into $\rho\pi$. Also the pole which is mainly A_1 must be associated with $q\bar{q}$, because it does not decay into $\epsilon\pi$. On the other hand, the remaining pole is more or less equally likely to decay into $\epsilon\pi$

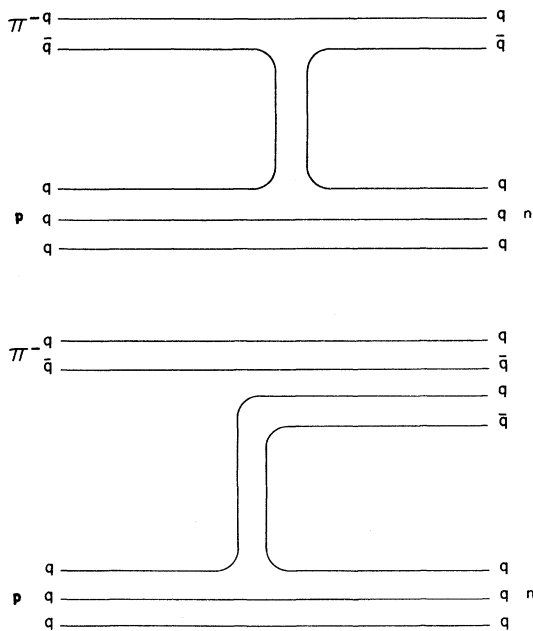


FIG. 1. Quark diagram for charge-exchange reactions $\pi^- p \rightarrow n q \bar{q}$ and $\pi^- p \rightarrow n 2q 2\bar{q}$.

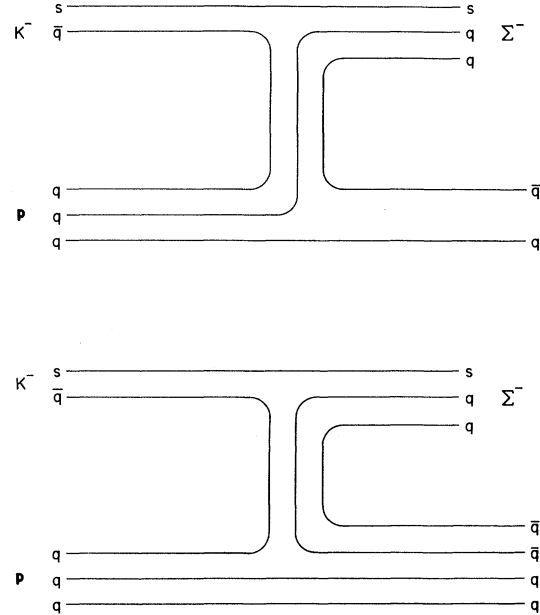


FIG. 2. Quark diagram for backward-production reactions $K^- p \rightarrow \Sigma^- q \bar{q}$ and $K^- p \rightarrow \Sigma^- 2q 2\bar{q}$.

and $\rho\pi$; thus it should be associated with a $2q2\bar{q}$ state.

In the last paragraph we have associated the three K -matrix poles with $q\bar{q}$, $2q2\bar{q}$, and $3q3\bar{q}$ states. Since the ρ only couples to the first two poles and the ϵ couples to the last two, we can drop these zero couplings without changing our fit. For the CEX and the BEX only $q\bar{q}$ and $2q2\bar{q}$ arrangements are possible; see Figs. 1 and 2. These diagrams further reduce the number of parameters in the BEX from six to four (CEX already had been cut down to two by the ρ -exchange assumption). We can further reduce the BEX parameters by one when we realize that no phase information makes it possible to choose one of the C_i^{BEX} parameters real.

Let us turn our attention to the ACCMOR data and their production mechanism. Here we clearly need production of $3q3\bar{q}$ in order to explain the $\epsilon\pi$ amplitude. Diffractive production proceeds by Pomeron exchange. It has become fashionable to think of the Pomeron as the vacuum realization of the 0^{++} two-gluon glueball state. A 0^{++} state will couple to either $q\bar{q}$ in a P wave or $2q2\bar{q}$ in an S wave state. The four possible diagrams are shown in Fig. 3. Thus one must retain all 12 parameters for Pomeron or diffractive production. In examining Figs. 2 and 3 one should note that another BEX diagram is possible which leads to a $3q3\bar{q}$. Since in this diagram the lower $3q$ state is

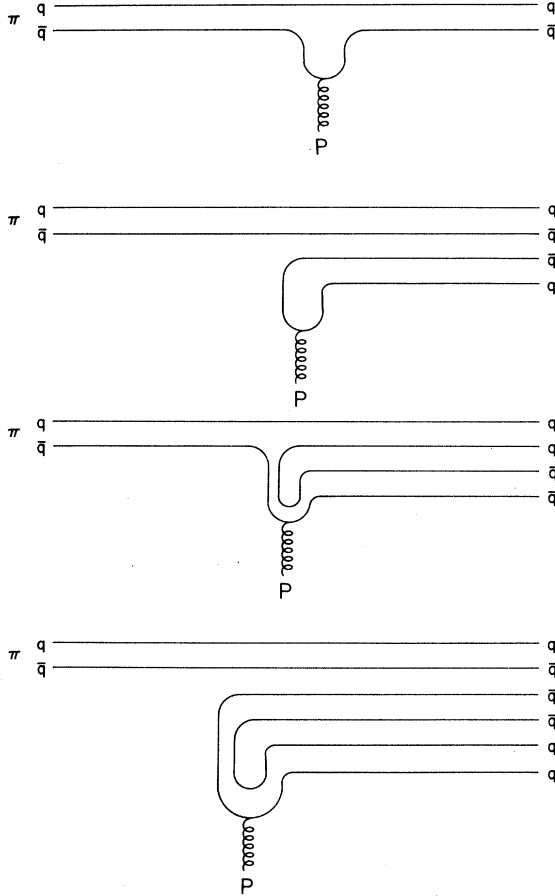


FIG. 3. Quark diagram for diffractive production reactions. The Pomeron (P) couples to either $q\bar{q}$ in a P -wave state or $2q2\bar{q}$ in an S -wave state.

initially associated with a baryon and must retain its identity until after the antibaryon is exchanged, we do not expect this to contribute until after the baryon/antibaryon threshold around 2.0 GeV.

The final number of parameters used in the fit

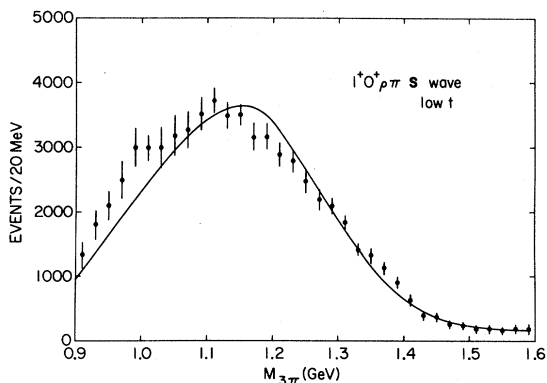


FIG. 4. ACCMOR (low t), $J^P M^\eta=1^+0^+$ $\rho\pi$ S -wave cross section. Fit described in the main text, Sec. III.

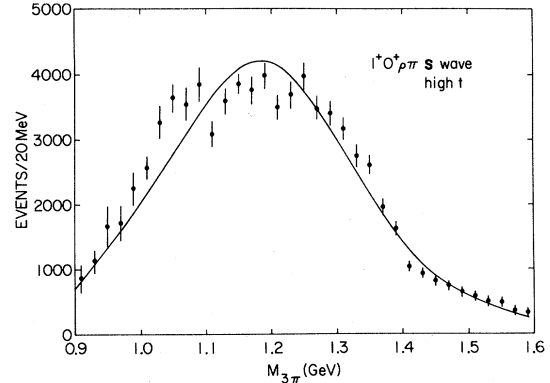


FIG. 5. ACCMOR (high t), $J^P M^\eta=1^+0^+$ $\rho\pi$ S -wave cross section.

goes from 29 down to 24. The number of data points in the ACCMOR LT is equal to 130 with an equal amount in the ACCMOR HT. The ACCMOR amplitudes account for 260 data points, while the CEX amplitudes have 48 data points with the BEX only adding 5 more points. This leaves us with a grand total of 291 DF (degrees of freedom) in the fit. The χ^2 which is obtained in the final fit comes to 477.4. Figures 4 through 11 show the fit for ACCMOR, CEX, and BEX. One can see in Fig. 11 that we do a very good job at reproducing a low-mass bump. The BEX has 6.9 times as much $2q2\bar{q}$ state produced as the CEX. Note in Fig. 11 that the predicted phase motion is quite large. One observes that the BEX taken in isolation of the other reactions would be consistent with a 1070 MeV mass A_1 with a 300 MeV width and expected phase motion. We believe that the so-called low-mass backward-produced A_1 is an effect caused by strong $q\bar{q}$ and $2q2\bar{q}$ interference. We would like to encourage more experiments on the BEX in order to help confirm or disprove our model.

In an earlier paper⁵ we had fit the ACCMOR

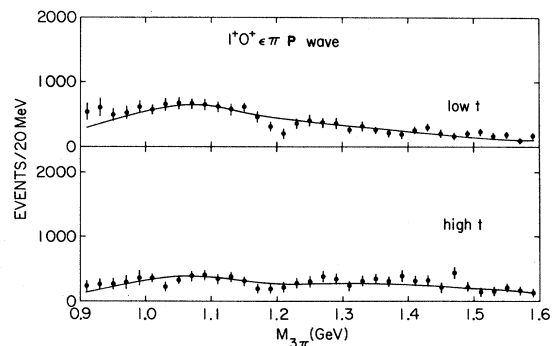


FIG. 6. ACCMOR (low t and high t), $J^P M^\eta=1^+0^+$ $\epsilon\pi$ P -wave cross sections.

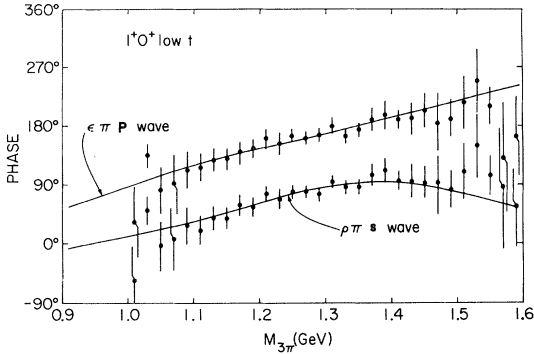


FIG. 7. ACCMOR (low t), $J^P M^\eta = 1^+ 0^+$ $\rho\pi$ S-wave and $\epsilon\pi$ P-wave phases.

and CEX data. In that paper, we followed the philosophy of having the Deck-type production only in the P vector and not in the K matrix. However, the CEX data have a peak which is lower in mass than the $q\bar{q}A_1$ mass and no $\epsilon\pi$ amplitude at all (see Fig. 9). As in this paper the CEX data represented $\rho\pi$ scattering thus requiring the addition of another pole in the K matrix. In Ref. 5, we noted that this pole could be equally described by a (charge-exchange but “Deck-like”) multi-Regge background as done in Ref. 2. We had argued that this approach and ours are dual to each other. To the extent that CEX represents $\rho\pi$ scattering all poles should go into the K matrix. With this additional pole in the K matrix, the $\epsilon\pi$ amplitude of ACCMOR now had the two-component structure necessary to explain data (except near threshold). This two-component structure in the $\epsilon\pi$ amplitude could not come from the A_1 (as in Ref. 8) because of the lack of $\epsilon\pi$ in CEX. The $\rho\pi$ amplitude of ACCMOR already had the $\rho\pi$ Deck effect to shift its mass and thus necessarily reduced (compared to CEX) the coupling of the second K -matrix pole in ACCMOR. The possibili-

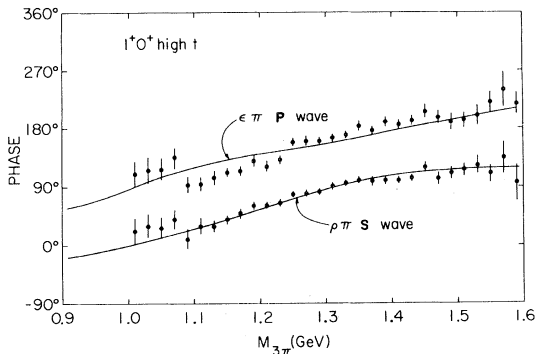


FIG. 8. ACCMOR (high t), $J^P M^\eta = 1^+ 0^+$ $\rho\pi$ S-wave and $\epsilon\pi$ P-wave phases.

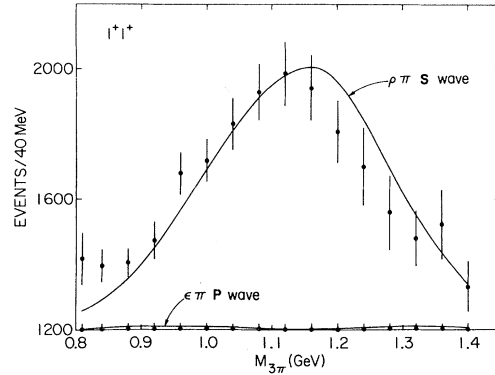


FIG. 9. CEX, $J^P M^\eta = 1^+ 1^+$ $\rho\pi$ S-wave and $\epsilon\pi$ P-wave cross sections.

ty that this second K -matrix pole could be dual to the Deck amplitude in the diffractive channel was the main motive for the present paper.

Let us compare the approach of placing the Deck amplitudes in the P vector only⁵ to the present work. Our present fit has 291 DF and a χ^2 of 477.4 or χ^2/DF of 1.64. The P -vector Deck approach has 282 DF with a χ^2 of 683.1 (or $\chi^2/\text{DF} = 2.42$). It is true this paper considers BEX, adding 2 DF, but this is only a 1% effect. The reason the Deck fit had such a bad χ^2 was entirely due to the $\epsilon\pi$ ACCMOR data near threshold. The $\epsilon\pi$ ACCMOR amplitudes (see Figs. 6 and 8) have phase motion near threshold, which cannot be attributed to the A_1 resonance, because there is no $\epsilon\pi$ amplitude in the CEX data. In Ref. 5 we resorted to an admittedly *ad hoc* procedure of introducing rescattering effects into the Deck amplitudes alone. For these rescattering effects we used the results of Ref. 8. This introduced the desired phase motion without changing the rest of the fit and χ^2 fell from 683.1 and 460.9 (or $\chi^2/\text{DF} = 1.63$). In retrospect, one must admit that rescattering is more than a kinematic effect and is related to underlying

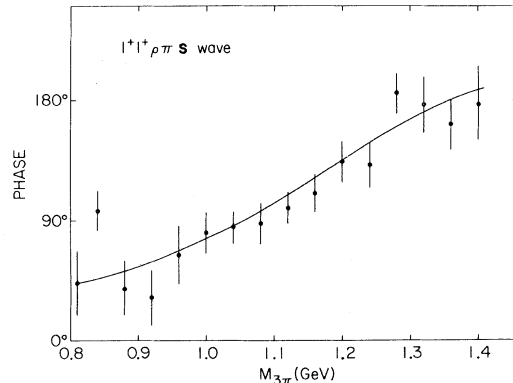


FIG. 10. CEX, $J^P M^\eta = 1^+ 1^+$ $\rho\pi$ S-wave phase.

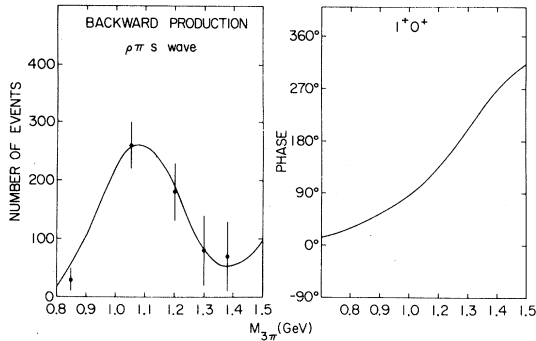


FIG. 11. BEX, $J^P M^\eta=1^+0^+$ $\rho\pi$ S -wave cross section. The phase is predicted by the fit described in Sec. III of the main text.

dynamics. The purpose of a K -matrix pole is to introduce dynamical behavior that cannot be attributed to kinematics. Thus Ref. 5 in a way had introduced a K -matrix pole which created phase motion in the $\epsilon\pi$ channel alone. The most important aspect of the 3π data coming from Refs. 2–4 is the decoupling of $\rho\pi$ scattering from $\epsilon\pi$ scattering. This is the major reason Ref. 8 went so wrong and all other analyses that assumed $\epsilon\pi$ was unimportant went so right (Refs. 6 and 7). We believe that the present work isolates the underlying dynamics into three K -matrix poles which can be interpreted in terms of quark states ($q\bar{q}$, $2q2\bar{q}$, and $3q3\bar{q}$), where other exchange (Deck effect) and re-scattering effects are a dual approach which gives an equally good fit. Table I gives the K -matrix pole parameters that were obtained in the three-pole fit. However as discussed in Ref. 1 the K -matrix poles are not equal to the poles of the S matrix. In the Appendix we have derived a relationship between the K matrix and Breit-Wigner parameters based on a method of Goebel and McVoy.¹¹ This method gives an exact prescription of how one K -matrix pole shifts the derived Breit-Wigner parameters of the other K -matrix pole. In our case we have three poles and are interested in the Breit-Wigner parameters of one in the presence of the other two. In order to obtain a better understanding of how the poles affect each other,

we first consider the interaction of only two of the poles. The first entry in Table I is the A_1 K -matrix pole which only couples to the $\rho\pi$ channel. The first entry in Table II shows the effect of second K -matrix pole ($2q2\bar{q}$) using Eqs. (A22) and (A23) of the Appendix. Since the second pole couples to both $\rho\pi$ and $\epsilon\pi$, we have picked up a 4% coupling of the A_1 to $\epsilon\pi$. The third K matrix ($3q3\bar{q}$) which only couples to $\epsilon\pi$ reduces the $\epsilon\pi$ coupling of the A_1 by a factor of 10 [using Eqs. (A26) and (A27) of the Appendix]. A similar effect takes place for the third pole in the presence of the second and then the first and second pole. The final Breit-Wigner parameters are completely decoupled such that $\rho\pi$ scattering only gives a $\rho\pi$ final state and $\epsilon\pi$ scattering only gives an $\epsilon\pi$ final state for the $J^P=1^+$ partial wave.

IV. SUMMARY

The analysis presented in this paper has shed light on two outstanding questions of the A_1 system: Why does the A_1 production cross section peak up at lower mass (~ 1100 MeV) in almost all reactions (except high- t diffractive production), while detail analysis gives a higher A_1 mass, 1250 MeV? What is the true nature of the so-called Deck mechanism⁹ and can one unify its treatment with the production of quark states? All previous analyses^{5–8} have answered the first question by introducing a background (the Deck mechanism) which interferes with the A_1 resonance and causes a shift in the 1250-MeV mass peak of the A_1 to lower masses. In this work we have argued that the Deck mechanism is dual to the direct production of a very broad $2q2\bar{q}$ state proposed by Jaffe.¹⁰ The fact that the interference is such that it shifts the mass always in the same way is a fundamental property of $\rho\pi$ scattering itself in the $J^P=1^+$ channel. The backward production⁴ of the $\rho\pi$ system shows a dramatic mass shift which is anticipated by the quark diagrams of Fig. 2. These diagrams demonstrate that baryon exchange leads naturally to the production of $2q2\bar{q}$ states. We have

TABLE I. The three K -matrix poles (in MeV units).

Type	Mass	$\Gamma_{\rho\pi}$	$\Gamma_{\epsilon\pi}$
$q\bar{q}$	1180 ± 30	290 ± 60	
$2q2\bar{q}$	5000 ± 2000	8000 ± 4000	2000 ± 1000
$3q3\bar{q}$	1180 ± 60		420 ± 80

TABLE II. Two different sets of Breit-Wigner parameters (in MeV units).

Type	Background	Mass	$\Gamma_{\rho\pi}$	$\Gamma_{\epsilon\pi}$
$q\bar{q}$	$2q2\bar{q}$	1230 ± 30	325 ± 60	12 ± 10
$q\bar{q}$	$2q2\bar{q} + 3q3\bar{q}$	1230 ± 30	330 ± 60	1 ± 1
$3q3\bar{q}$	$2q2\bar{q}$	1190 ± 60	9 ± 10	511 ± 90
$3q3\bar{q}$	$2q2\bar{q} + q\bar{q}$	1200 ± 60	0.1 ± 1	530 ± 90

also shown the $J^P = 1^+ \epsilon\pi$ scattering is completely orthogonal to $\rho\pi$ scattering, thus explaining why analyses which ignored this channel still achieved the correct answer. On the other hand, the one analysis⁸ which required the $\epsilon\pi$ channel to couple to the A_1 resonance gave a wrong result for the mass of the A_1 and predicted that $\rho\pi$ scattering would lead to large amount of $\epsilon\pi$ production. This possibility is excluded by the CEX data.³

Finally, the generalized Watson theorem first developed by Aitchison can be applied to other production processes that may contain multi-quark states which in general appear to be very broad. This feature arises from the superallowed decay modes in which color-singlet subunits fall apart without feeling an overall confining force.¹² In order to compare these states with theory, one would have to resort to methods derived in Ref. 12 and applied in Refs. 5 and 12.

ACKNOWLEDGMENTS

I would like to thank M. G. Bowler for suggesting that the Deck mechanism would be equivalent to a four-quark interaction. I also would like to thank I. J. R. Aitchison for the simple but elegant formalism on which this work is based. This work was performed under the auspices of the United States Department of Energy under Contract No. DE-AC02-76CH00016.

APPENDIX: A RELATIONSHIP BETWEEN THE K -MATRIX POLES AND BREIT-WIGNER PARAMETERS

In this appendix we present a relationship between the K -matrix poles as introduced in the main text and Breit-Wigner resonance parameters. This

relationship is achieved using Ref. 11 in which one focuses on the situation of an isolated resonance in the presence of a background. All the formulas in this appendix will be based on a simple single-channel elastic π - π scattering. The final part of the Appendix will generalize to the multichannel case with two K -matrix poles as part of the background parametrization.

The partial wave cross section for π - π scattering in a given angular momentum state l is related to the T matrix by

$$\sigma_l = \frac{4\pi}{k^2} (2l+1) |T_l|^2, \quad (\text{A1})$$

where k is the center-of-mass momentum of one π in the appropriate units. The K matrix as introduced in the main text is related to the above T matrix by

$$T_l = (1 - iK_l)^{-1} K_l. \quad (\text{A2})$$

The T matrix written in terms of a single-channel relativistic Breit-Wigner form is given by

$$T_l = \frac{m\Gamma}{m^2 - s - im\Gamma}. \quad (\text{A3})$$

The above two equations lead to the K matrix being written as

$$K_l = \frac{m\Gamma}{m^2 - s}. \quad (\text{A4})$$

For the remainder of the Appendix we will drop the subscripted l . If two poles occur in the K matrix, then Eq. (A4) becomes

$$K = \frac{m_1\Gamma_1}{m_1^2 - s} + \frac{m_2\Gamma_2}{m_2^2 - s}. \quad (\text{A5})$$

Substituting this K matrix into Eq. (A2) we obtain

$$T = \frac{m_1\Gamma_1(m_2^2 - s - im_2\Gamma_2) + m_2\Gamma_2(m_1^2 - s - im_1\Gamma_1) + 2im_1m_2\Gamma_1\Gamma_2}{(m_1^2 - s - im_1\Gamma_1)(m_2^2 - s - im_2\Gamma_2) + m_1m_2\Gamma_1\Gamma_2}. \quad (\text{A6})$$

Equation (A6) is quite messy and tends to obscure the relationship we wish to obtain. We can achieve a simplification by defining three new symbols,

$$U_j = (m_j \Gamma_j)^{1/2}, \quad (\text{A7})$$

$$D_{jk} = i(m_j \Gamma_j m_k \Gamma_k)^{1/2}, \quad (\text{A8})$$

and

$$D_j = m_j^2 - s - im_j \Gamma_j. \quad (\text{A9})$$

Equation (A3), the relativistic Breit-Wigner form, would then be written as

$$T = \frac{m \Gamma}{m^2 - s - im \Gamma} = \frac{UU}{D}, \quad (\text{A10})$$

and Eq. (A6) is simplified to

$$T = \frac{U_1 D_2 U_1 + U_2 D_1 U_2 + 2U_1 D_{12} U_2}{D_1 D_2 - D_{12}^2}. \quad (\text{A11})$$

We are now in the position to make a connection with the above K -matrix formalism and Ref. 11. In Ref. 11 it is assumed that a smooth unitary background exists and can be parametrized by some well defined procedure. In our case we will choose one of the K -matrix poles to describe our background. When a resonance is introduced into the above-mentioned situation, Ref. 11 shows that it takes the form

$$T_R = \frac{m \Gamma e^{2i\theta}}{m^2 - s - im \Gamma}, \quad (\text{A12})$$

where θ is a function of energy and depends on the background parametrization. We can achieve exactly this solution if we rewrite Eq. (A11) as

$$T = \frac{U_1 U_1}{D_1} + \frac{(D_2 + D_{12} U_1 / D_1)(U_2 + D_{12} U_1 / D_1)}{D_2 - D_{12}^2 / D_1}. \quad (\text{A13})$$

In our case the second term in Eq. (A13) is equivalent to Eq. (A12); thus

$$m^2 - s - im \Gamma = D_2 - \frac{D_{12}^2}{D_1}, \quad (\text{A14})$$

$$m \Gamma = \left| U_2 + \frac{D_{12} U_1}{D_1} \right|^2, \quad (\text{A15})$$

and

$$e^{2i\theta} = \frac{(U_2 + D_{12} U_1 / D_1)^2}{|U_2 + D_{12} U_1 / D_1|^2}. \quad (\text{A16})$$

We can easily generalize the above set of equa-

tions to the multichannel problem by introducing the concept of partial widths into the channels a , b , c , etc. The total width is defined as the sum of the partial widths over all open channels for the j th K -matrix pole

$$\Gamma_j = \sum_a \Gamma_{ja}. \quad (\text{A17})$$

Equation (A7) then becomes

$$U_{ja} = \pm (m_j \Gamma_{ja})^{1/2}, \quad (\text{A18})$$

where the plus or minus depends on the sign of the coupling.

Equation (A13) is now written as

$$T_{ab} = \frac{U_{1a} U_{1b}}{D_1} + \frac{\left[U_{2a} + D_{12} U_{1a} / D_1 \right] \left[U_{2b} + D_{12} U_{1b} / D_1 \right]}{D_1 - D_{12}^2 / D_1}. \quad (\text{A19})$$

Reference 11 writes the multichannel resonance in the form

$$T_{ab}^R = \frac{m \Gamma_a^{1/2} \Gamma_b^{1/2} e^{i\theta_a} e^{i\theta_b}}{m^2 - s - im \Gamma}, \quad (\text{A20})$$

where

$$\Gamma = \sum_a \Gamma_a. \quad (\text{A21})$$

Relating the second term in Eq. (A19) with Eq. (A20), we obtain

$$m^2 - s - im \Gamma = D_2 - \frac{D_{12}^2}{D_1}, \quad (\text{A22})$$

$$m \Gamma_a = \left| U_{2a} + \frac{D_{12} U_{1a}}{D_1} \right|^2, \quad (\text{A23})$$

and

$$e^{i\theta_a} = \frac{(U_{2a} + D_{12} U_{1a} / D_1)}{U_{2a} + D_{12} U_{1a} / D_1}. \quad (\text{A24})$$

In the final part of this appendix we will write down the analogous equations [Eqs. (A22)–(A24)] for a background made up of two K -matrix poles. Equation (A19) for three K -matrix poles becomes

$$\begin{aligned}
T_{ab} = & \frac{U_{1a}D_2U_{1b} + U_{2a}D_1U_{2b} + U_{1a}D_{12}U_{2b} + U_{2a}D_{12}U_{1b}}{D_1D_2 - D_{12}^2} \\
& + \left\{ \left[U_{3a} + \frac{D_1D_{23} + D_{12}D_{13}}{D_1D_2 - D_{12}^2} \right] U_{2a} + \frac{D_2D_{13} + D_{12}D_{23}}{D_1D_2 - D_{12}^2} \right] U_{1a} \right\} \\
& \times \left\{ \left[U_{3b} + \frac{D_1D_{23} + D_{12}D_{13}}{D_1D_2 - D_{12}^2} \right] U_{2b} + \frac{D_2D_{13} + D_{12}D_{23}}{D_1D_2 - D_{12}^2} \right] U_{1b} \right\} \Big/ D_3 - \frac{D_1D_{23}^2 + D_2D_{13}^2 + 2D_{12}D_{23}D_{13}}{D_1D_2 - D_{12}^2},
\end{aligned} \tag{A25}$$

therefore

$$m^2 - s - im\Gamma = D_3 - \frac{D_1D_{23}^2 + D_2D_{13}^2 + 2D_{12}D_{23}D_{13}}{D_1D_2 - D_{12}^2}, \tag{A26}$$

$$m\Gamma_a = \left| U_{3a} + \frac{D_1D_{23} + D_{12}D_{13}}{D_1D_2 - D_{12}^2} \right] U_{2a} + \frac{D_2D_{13} + D_{12}D_{23}}{D_1D_2 - D_{12}^2} \right] U_{1a} \right|^2, \tag{A27}$$

and

$$e^{i\theta_a} = \frac{U_{3a} + \frac{D_1D_{23} + D_{12}D_{13}}{D_1D_2 - D_{12}^2} \right] U_{2a} + \frac{D_2D_{13} + D_{12}D_{23}}{D_1D_2 - D_{12}^2} \right] U_{1a}}{\left| U_{3a} + \frac{D_1D_{23} + D_{12}D_{13}}{D_1D_2 - D_{12}^2} \right] U_{2a} + \frac{D_2D_{13} + D_{12}D_{23}}{D_1D_2 - D_{12}^2} \right] U_{1a} \right|}. \tag{A28}$$

¹I. J. R. Aitchison, Nucl. Phys. **A189**, 417 (1972).

²Amsterdam-CERN-Crakow-Munich-Oxford-Rutherford Collaboration (hereafter referred to as ACCMOR), Phys. Lett. **89B**, 281 (1980). The latter reference contains only the $1^+ \rho\pi$ data. The $1^+ \epsilon\pi$ diffractive data was provided by the ACCMOR collaboration (private communication).

³Carleton-McGill-Ohio State-Toronto Collaboration (hereafter referred to as CEX), Phys. Rev. Lett. **46**, 580 (1981).

⁴CERN-Amsterdam-Nijmegen-Oxford Collaboration (hereafter referred to as BEX), Phys. Lett. **69B**, 119 (1977).

⁵R. Aaron and R. S. Longacre, Phys. Rev. D **24**, 1207

(1981).

⁶J. L. Basdevant and E. L. Berger, Phys. Rev. D **16**, 657 (1977).

⁷M. G. Bowler, M. A. V. Game, I. J. R. Aitchison, and J. B. Dainton, Nucl. Phys. **B97**, 227 (1975).

⁸R. Aaron, R. S. Longacre, and J. E. Sacco, Ann. Phys. (N.Y.) **117**, 56 (1979).

⁹The Deck background mechanism was first discussed by R. T. Deck, Phys. Rev. Lett. **13**, 169 (1964).

¹⁰R. L. Jaffe, Phys. Rev. D **15**, 267 (1977).

¹¹C. J. Goebel and K. W. McVoy, Phys. Rev. **164**, 1932 (1967).

¹²R. L. Jaffe and F. E. Low, Phys. Rev. D **19**, 2105 (1979).